Three-dimensional phase-field simulation of domain structures in ferroelectric islands

J. X. Zhang,[1,a)] R. Wu,[1] S. Choudhury,[1] Y. L. Li,[1] S. Y. Hu,[2] and L. Q. Chen[1]
[1]*Department of Materials Science and Engineering, Pennsylvania State University, University Park, Pennsylvania 16802, USA*
[2]*Pacific Northwest National Laboratory, Richland, Washington, 99352, USA*

(Received 24 January 2008; accepted 2 March 2008; published online 26 March 2008)

A three-dimensional phase-field model was developed for studying domain structures in ferroelectric islands attached onto a substrate. It simultaneously takes into account the long-range electric and elastic interactions, substrate constraint, as well as the stress relaxation caused by the surfaces of an island. The phase-field simulations demonstrated that the domain structures of ferroelectric islands could be dramatically different from those of continuous thin films due to the change of stress state. The stress distribution inside islands is highly dependent on the aspect ratio of the islands. It provides us an effective way for engineering the domain structures of ferroelectric materials. © *2008 American Institute of Physics*. [DOI: 10.1063/1.2903107]

Ferroelectrics are a class of functional materials that are attractive for a variety of applications due to their superior piezoelectric, dielectric, and pyroelectric properties. Many applications such as silicon-based microelectromechanical system sensor and actuator applications require the fabrication of ferroelectric materials in the form of thin films on a substrate.[1] While the substrate constraint may lead to dramatic increases in a number of ferroelectric properties including the transition temperatures, it may significantly suppress other properties such as the piezoelectric responses of a thin film.[2–5] However, it has been shown that additional manipulation of the properties of a thin film is possible through patterning. For example it is demonstrated, both theoretically and experimentally,[6–11] that the substrate clamping could be reduced by cutting the ferroelectric thin film into isolated islands using, e.g., focused ion-beam patterning,[7,8] photolithography,[12] or electron-beam lithography,[6] leading to enhanced piezoelectric responses as compared to a continuous film.

One of the keys to predicting the ferroelectric/piezoelectric properties of an island is the fundamental understanding of how domain structures in the ferroelectric thin film are affected by patterning. Baik and co-workers,[13,14] found that the volume fraction of *c* domains in an epitaxial $PbTiO_3$ island changes with its aspect ratio. Fu and co-workers,[15,16] studied the domain structures and the depolarization effect in ferroelectric nanostructures using a first-principles-derived effective Hamiltonian approach. Wang and Zhang[17] studied the domain configuration and polarization switching in islands by using a phase-field model in two dimensions.

The main purpose of this paper is to develop a three-dimensional phase-field model for predicting the domain structures of ferroelectric islands. The model simultaneously takes into account the long-range interactions such as electric and elastic interactions, substrate constraint, as well as the stress relaxation caused by the surfaces of an island. As an example, we study the domain structures of $PbZr_{0.2}Ti_{0.8}O_3$ ferroelectric islands. Our focus is on the difference in the inhomogeneous stress distributions between isolated islands and continuous thin films and its effect on the ferroelectric domain structures. The effect of electric boundary conditions on the domain structures will also be discussed.

In order to describe the ferroelectric transition and domain structures using the phase-field model, a local spontaneous polarization field $\mathbf{P}=(P_1,P_2,P_3)$ is chosen as the field variable. The temporal domain structure evolution is described by the time-dependent Ginzburg–Landau equation (TDGL),

$$\frac{\partial P_i}{\partial t} = -L\frac{\delta F}{\delta P_i} \quad (i=1,2,3), \tag{1}$$

where L is a kinetic coefficient that is related to the domain evolution and F is the total free energy of the system, which is expressed by

$$F = F_{\text{bulk}} + F_{\text{wall}} + F_{\text{elec}} + F_{\text{elas}}, \tag{2}$$

where F_{bulk}, F_{wall}, F_{elec}, and F_{elas} are bulk free energy, domain wall energy, electrostatic energy, and elastic energy, respectively. The mathematical expressions for these energy terms are exactly the same as those given in Ref. 18.

The electrostatic energy of an isolated island, for the case of open-circuit boundary condition, i.e., the polarization charges at the surfaces of an island are not compensated, can be calculated from a convolution of the polarization with the three-dimensional LaBonte interaction matrix,[19,20] which can be efficiently evaluated using fast Fourier transform techniques. To calculate the elastic energy for an isolated island, we present the model using three phases, i.e., a gas, an island, and a substrate, as shown in Fig. 1(a). The elastic solution for such system can be obtained by using the iteration method developed for elastic inhomogeneous systems[21,22] and the stress-free boundary conditions along the surfaces of an island can be automatically satisfied by setting the elastic constants as zero for the gas phase.

The temporal evolution of the polarization field and thus the domain structures are obtained by numerically solving the TDGL equations using the semi-implicit Fourier spectral method.[23] In the computer simulation, we employed a model of $128\Delta x \times 128\Delta x \times 64\Delta x$, and the thickness of the substrate

a)Electronic mail: jzz108@psu.edu.

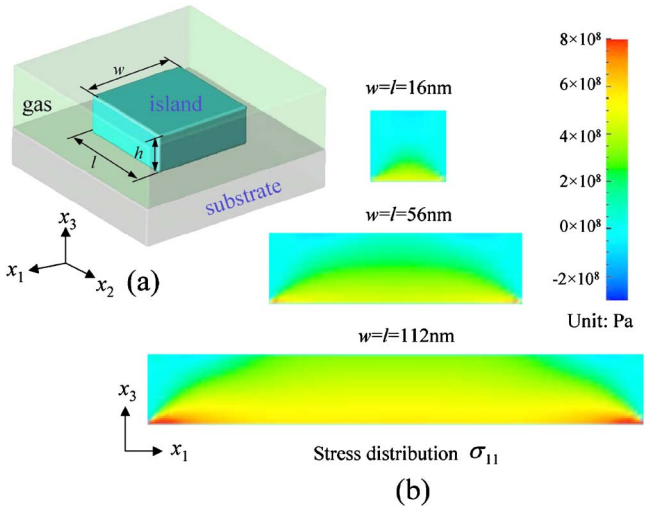

FIG. 1. (Color online) (a) Schematic illustration of a ferroelectric island. (b) The in-plane stress σ_{11} distribution along the cross section at the center of the ferroelectric island (h=16 nm, e^0=0.005).

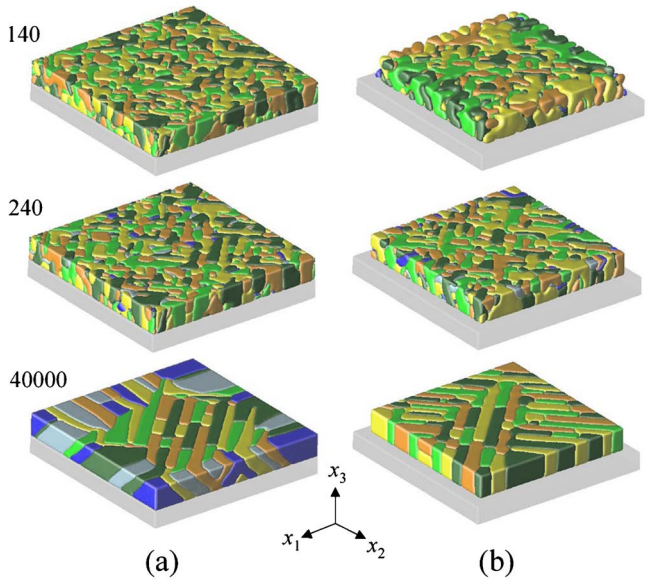

FIG. 2. (Color online) The temporal domain structure evolution of (a) a continuous thin film (h=16 nm) and (b) an isolated island (w=l=112 nm, h=16 nm). The different ferroelectric tetragonal variants are shown in different colors, i.e., yellow=$a_1^+([100])$, orange=$a_1^-([\bar{1}00])$, light green =$a_2^+([010])$, green=$a_2^-([0\bar{1}0])$, blue=$c^+([001])$, and light blue=$c^-([00\bar{1}])$. (e^0=0.005).

is taken as $h_s=30\Delta x$. The material constants for the Landau free energy and electrostrictive coefficients of $PbZr_{0.2}Ti_{0.8}O_3$ are listed in Ref. 24.[25] The cell size in real space is chosen to be $\Delta x=l_0$, where $l_0=\sqrt{G_{110}/\alpha_0}$ and $\alpha_0=|\alpha_1|_{T=25\,^\circ C}$. We chose the gradient energy coefficient as $G_{11}/G_{110}=0.6$. If l_0 =1.0 nm, $G_{110}=1.73\times10^{-10}$ C^{-2} m^4 N, and the corresponding wall thickness is about 1.5 nm. The initial polarization is created by assigning a zero value at each cell plus a small random noise.

It is known that, for the continuous thin films, their lateral lengths are constrained by the substrate, and the complete relaxation of the average in-plane stress requires that $\langle\varepsilon_{11}^0\rangle=\langle\varepsilon_{22}^0\rangle=e^0$, where $\langle\varepsilon_{ij}^0\rangle$ represents the volume average of stress-free strain ε_{ij}^0 over the film, and e^0 is the biaxial substrate strain. As a result, the volume fractions of different phases inside the film are essentially determined by the substrate strain. By cutting the film into isolated islands, the substrate constraint can be partially removed due to the generated free surfaces. To isolate the effect of the stress state on the domain structure of an island, we artificially removed the electrostatic energy in our first set of simulations. Figure 2 shows the temporal evolution of the domain structures of a ferroelectric island and a continuous thin film with same thickness and substrate strains (e^0=0.005). In the initial stage, for the thin film, the nucleation and growth of a_1/a_2 domain were observed, since the biaxial tensile substrate strain (stress) favors the a_1/a_2 domain energetically. However, for the thin films under a biaxial tensile substrate strain of 0.005, the stable domain structure contains all three types of domains, c, a_1, and a_2, due to the substrate constraint as we discussed above. Therefore, c domains nucleate in the later stage leading to a $c/a_1/a_2$ polytwin structure. On the other side, for the isolated island, a_1/a_2 domain was dominant in the initial stage, as the stress distribution inside the island is still mostly tensile except for the regions near the free surfaces as shown in Fig. 1(b), where a small amount of c domain was also observed. However, in the later stage, no nucleation of c domain was observed since the substrate constraint has been partially removed. It should be noted that along the island/substrate interface the substrate constraint still exists, and the nucleation of c domain would decrease the elastic energy locally but create additional domain wall energy. Since the domain wall energy penalty dominates, the c domain could not nucleate and even the pre-existed c domains along the free surfaces disappear. If we decrease the thickness of the island, as shown in Fig. 3(a), a $c/a_1/a_2$ polytwin domain structure was obtained as the elastic energy contribution along the island/substrate interface becomes dominant for this case.

The stress distribution inside islands is highly dependent on the aspect ratio, i.e., lateral dimension over island thickness $w(l)/h$. Figure 1(b) shows the in-plane stress σ_{11} distribution inside the islands with the same thickness but different lateral size $w(=l)$ under a biaxial tensile substrate strain e^0=0.005. For the stress calculation, the spontaneous polarization of islands was chosen to be zero, corresponding to a paraelectric phase. Dramatic changes in stress state were observed due to relaxation at the free surfaces. With the decrease of the lateral length of the island along x_1 axis (w), the average in-plane stress σ_{11} deceases and could eventually become almost zero. It should be noted that the in-plane stress σ_{22} also shows a similar dependence on the lateral length of the island along x_2 axis (l). Therefore, it provides us an effective way for engineering the domain structures of

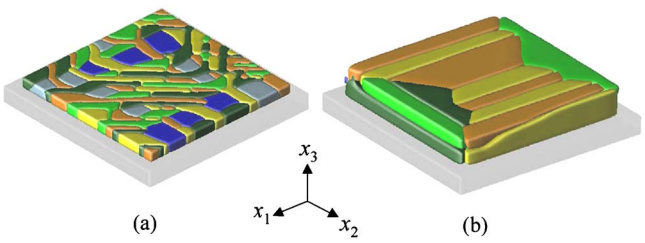

FIG. 3. (Color online) (a) The equilibrium domain structure of an isolated island without the electrostatic energy (w=l=112 nm, h=6 nm and e^0 =0.005). (b) The equilibrium domain structure of an isolated island with the electrostatic energy (w=l=112 nm, h=16 nm and e^0=0.005).

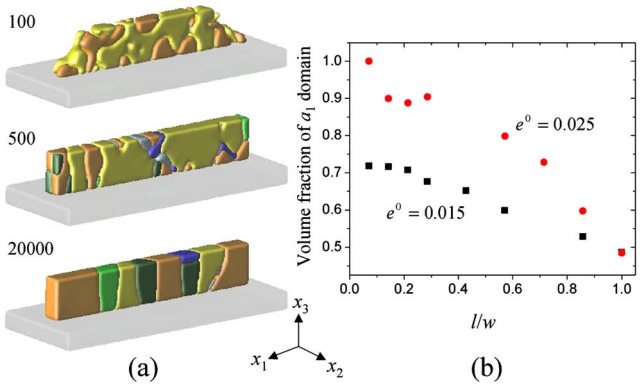

FIG. 4. (Color online) (a) The temporal domain structure evolution of an isolated island ($l/w=1/14$, $w=112$ nm, $h=20$ nm, $e^0=0.015$). (b) The volume fraction of a_1 domain as a function as the in-plane aspect ratio l/w ($w=112$ nm, $h=20$ nm).

ferroelectric materials. For example, we can create an anisotropic in-plane stress by controlling the relative in-plane length of the island (l/w), even under a biaxial substrate strain. For the islands shown as Fig. 4(a), the average in-plane tensile stress σ_{11} is larger than σ_{22} due to the unequal lengths of the island along x_1 and x_2 axis. As a result, when the sample was quenched to room temperature, only a_1 domains nucleate [Fig. 4(a)]. Although a small fraction of a_2 or c domains nucleates to relax the substrate constraint along the island/substrate interface in the later stage, the volume fraction of a_1 domain still dominates in the final domain structure. As shown in Fig. 4(b), we can effectively control the volume fraction of a_1 domain by the in-plane aspect ratio l/w, i.e., the volume fraction of a_1 domain is about 50% when the in-plane aspect ratio $l/w=1$, and it will increase with the decrease of the in-plane aspect ratio. It should be noted that we could also increase the volume fraction of a_2 domains by increasing the in-plane aspect ratio. It is even possible to obtain domain structures with 100% a_1 (or a_2) domains with higher substrate strains, which is important for piezoelectric applications.

The electrostatic energy that we have ignored so far is also expected to play an important role in the domain structures of ferroelectric islands, especially for the open-circuit boundary case in which large depolarization fields are generated by the uncompensated charges along island surfaces. Figure 3(b) shows the equilibrium domain structure of an island under the open-circuit boundary condition. To minimize the depolarization field induced by the uncompensated charges, the polarization tends to be parallel to the island surfaces. Therefore, a vortexlike domain structure was obtained.

In summary, we have developed a three-dimensional phase-field model for studying the domain structures and their evolution in ferroelectric islands. Our simulations showed that the domain structures could be dramatically modified by patterning of a continuous thin film into isolated islands. In addition, the stress distribution inside islands is highly dependent on the aspect ratio, which provides us an effective way for engineering the domain structures of ferroelectric materials. For example, we can obtain domain structures with 100 percent a_1 (or a_2) domains by controlling the in-plane aspect ratio of the islands. The electrostatic energy also has significant effect on the domain structures of ferroelectric islands under the open-circuit boundary condition.

The authors are grateful for the financial support by Department of Energy under the Grant No. DOE DE-FG02-07ER46417 and by the National Science Foundation under Grant Nos. DMR-0507146 and DMR 0708759.

[1] P. Muralt, J. Micromech. Microeng. **10**, 136 (2000).
[2] K. Leferi and G. J. M. Dormans, J. Appl. Phys. **76**, 1764 (1994).
[3] A. L. Kholkin, M. L. Galzada, P. Ramos, J. Mendiloa, and N. Setter, Appl. Phys. Lett. **69**, 3902 (1996).
[4] F. Xu, F. Che, and S. Trolier-McKinstry, J. Appl. Phys. **86**, 588 (1999).
[5] T. M. Shaw, S. Trolier-McKinstry, and P. C. McIntyre, Annu. Rev. Mater. Sci. **30**, 263 (2000).
[6] A. L. Roytburd, S. P. Alpay, V. Nagarajan, C. S. Ganpule, S. Aggarwal, E. D. Williams, and R. Ramesh, Phys. Rev. Lett. **85**, 190 (2000).
[7] S. Buhlmann, B. Dwir, J. Baborowski, and P. Muralt, Appl. Phys. Lett. **80**, 3195 (2002).
[8] V. Nagarajan, A. Stanishevsky, L. Chen, T. Zhao, B. T. Liu, J. Melngailis, A. L. Roytburd, and R. Ramesh, Appl. Phys. Lett. **81**, 4215 (2002).
[9] V. Nagarajan, A. Roytburd, A. Stranishevsky, S. Prasertchoung, T. Zhao, L. Chen, J. Melngailis, O. Auciello, and R. Ramesh, Nat. Mater. **2**, 43 (2003).
[10] V. Nagarajan, Appl. Phys. Lett. **87**, 242905 (2005).
[11] Z. Ma, F. Zavaliche, L. Chen, J. Ouyang, J. Melngailis, A. L. Royburd, V. Vaithyanathan, D. G. Schlom, T. Zhao, and R. Ramesh, Appl. Phys. Lett. **87**, 072907 (2005).
[12] K. Lee, K. Kim, S. J. Kwon, and S. Baik, Appl. Phys. Lett. **85**, 4711 (2004).
[13] K. Lee, H. Yi, W. H. Park, Y. K. Kim, and S. Baik, J. Appl. Phys. **100**, 051615 (2006).
[14] K. Lee and S. Baik, Annu. Rev. Mater. Sci. **36**, 81 (2006).
[15] I. I. Naumov, L. Bellaiche, and H. X. Fu, Nature (London) **432**, 737 (2004).
[16] I. Naumov and H. X. Fu, Phys. Rev. Lett. **98**, 077603 (2007).
[17] J. Wang and T. Y. Zhang, Phys. Rev. B **73**, 144107 (2006).
[18] Y. L. Li, S. Y. Hu, and L. Q. Chen, J. Appl. Phys. **97**, 034112 (2005).
[19] M. E. Schabes and A. Aharoni, IEEE Trans. Magn. **23**, 3882 (1987).
[20] R. H. Victora, IEEE Trans. Magn. **38**, 181 (2002).
[21] S. Y. Hu and L. Q. Chen, Acta Mater. **49**, 1879 (2001).
[22] P. Yu, S. Y. Hu, L. Q. Chen, and Q. Du, J. Comput. Phys. **208**, 34 (2005).
[23] L. Q. Chen and J. Shen, Comput. Phys. Commun. **108**, 147 (1998).
[24] $\alpha_1=3.44(T-456.4)\times10^5$ C^{-2} m^2 N, $\alpha_{11}=-3.05\times10^7$ C^{-4} m^6 N, $\alpha_{12}=6.32\times10^8$ C^{-4} m^6 N, $\alpha_{111}=2.48\times10^8$ C^{-6} m^{10} N, $\alpha_{112}=9.68\times10^8$ C^{-6} m^{10} N, $\alpha_{123}=-4.90\times10^9$ C^{-6} m^{10} N, $Q_{11}=0.081$ C^{-2} m^4, $Q_{12}=-0.024$ C^{-2} m^4, $Q_{44}=0.032$ C^{-2} m^4, $c_{11}=1.75\times10^{11}$ N m^{-2}, $c_{12}=0.794\times10^{11}$ N m^{-2}, $c_{44}=1.11\times10^{11}$ N m^{-2}, and $T=25$ °C.
[25] M. J. Haun, E. Furman, S. J. Jang, H. A. Mckinstry, and L. E. Cross, J. Appl. Phys. **62**, 3331 (1987).